

# ANIMA Collar Tag Sensor Calibrations and Power Management

Sarah Dean<sup>1</sup>, Max Dunne<sup>2</sup>, Gabriel Elkaim<sup>2</sup>

<sup>1</sup>University of Pennsylvania, <sup>2</sup>University of California Santa Cruz  
University of California Santa Cruz Autonomous Systems Lab

**Abstract**— GPS tracking collars, the current method of noninvasively studying large mammals, give limited and undetailed data. The ANIMA project seeks to improve upon tracking collars by creating a tag that integrates a GPS with a magnetometer and an accelerometer. The additional sensors will give information about animal physiology and daily behaviors. To remain a commercially viable option to research scientists, the ANIMA tag must have a long life deployment while operating on limited battery capacity. Therefore, the onboard sensors must work in the most energy efficient way possible. This project focused on characterizing the sensors. Their long term stability was characterized, their start-up times were measured, and their power consumption in various settings was determined. Using the information gathered, the sensors can be optimized for both energy use and performance.

**Keywords**—*accelerometer; magnetometer; GPS; current draw; stability*

## I. INTRODUCTION

Studying large terrestrial mammals is relevant for wildlife conservation and management because large mammals can have an important impact on the ecosystems in which they live. Important insights can be gained by understanding their physiological capacities and daily behaviors. The current non-invasive method of studying these animals is through the use of GPS tracking collars, which give limited and undetailed data.

The ANIMA (Accelerometer Network Integrator for Mobile Animals) project, a partnership between the departments of Computer Engineering, Ecology and Evolutionary Biology, and Environmental Studies at UC Santa Cruz, seeks to improve the current tracking collar technology. They are designing and creating a technologically advanced tag that integrates several sensors and will be able to collect detailed data on animal movement and behaviors. The sensors include a GPS, an accelerometer, and a magnetometer. The Mediatek-3329 GPS will be used to track location. The Freescale MMA8451Q accelerometer detects motion and can consequently determine information like step rate, approximate speed, and various behaviors ranging from sleeping to hunting. The Freescale MAG3110 magnetometer will measure direction. In conjunction with information from the accelerometer, the magnetometer can be used in dead-reckoning of position when the GPS is not in use for power saving reasons.

These sensors have unknown stabilities, start up times, and power consumptions. In order to collect data that is both

accurate and comprehensive while remaining energy efficient, these parameters must be characterized.

## II. STABILITY

All sensors inherently have noise, and this noise is dealt with in data processing algorithms. To test these algorithms, it is necessary to have accurate models of the sensor's noise. Using models, it is possible to compare the 'true signal' with the processed signal to optimize processing algorithms. The model used is

$$y_m = ky_t + b(t) + v_w \quad (1)$$

where  $y_m$  is the measured output of the sensor,  $y_t$  is the true signal,  $k$  is a scalar constant,  $v_w$  is the normally distributed wide band noise, and  $b(t)$  is a null shift that changes with time. This null shift is described by

$$db/dt = -(1/\tau)b + \omega \quad (2)$$

where  $\omega$  is normally distributed and  $\tau$  is a time constant.

An important case for this model occurs when the true signal is constant. Under these conditions, all the variation in the data is a result of the variation in the noise, since there is no variation in the true signal. Analyzing data taken with a known constant true signal can quantify the parameters of different types of noise, using the method of overbounding [1].

For this reason, data was collected from the magnetometer and accelerometer on long term runs in quiet environments. The data presented here is from two overnight runs, where data from the sensors was collected at 5 Hz. The accelerometer's output data rate was set to 6.25 Hz, and the magnetometer's was set at 10 Hz with an oversample ratio of 128. Data from the magnetometer was observed to drift and show effects of nearby electronics, so magnetometer samples were clipped to the relatively more stable portions.

The parameters of the noise were characterized using autocorrelation and an Allan variance analysis, following the method of overbounding[1]. Fig. 1 shows an example of the Allan variance plot and the autocorrelation plot for one axis of the accelerometer. Fig. 2 shows another example of these plots for the magnetometer. In the case of Fig. 2, the technique does not work because the magnetometer data was correlated.

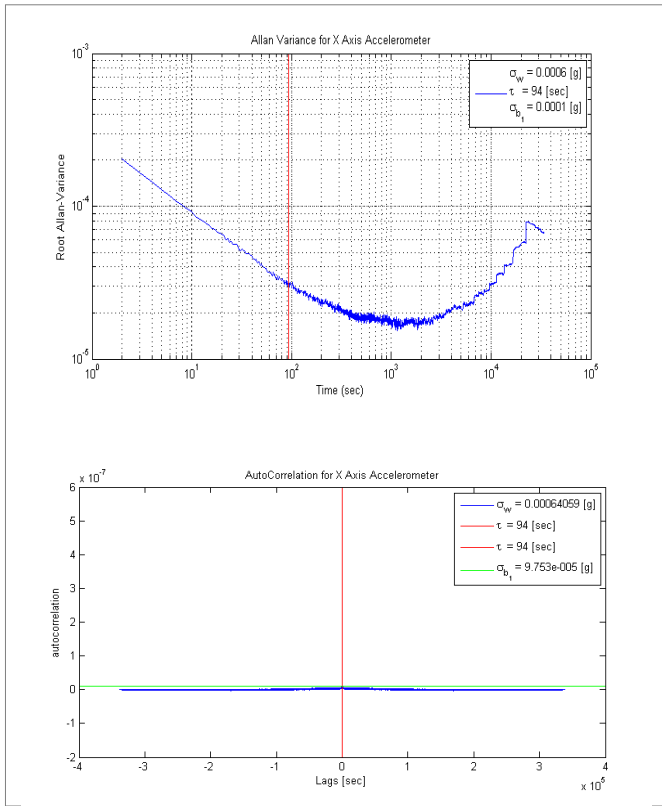


Fig. 1. The Allan variance plot and the autocorrelation plot generated in the overbounding analysis of the accelerometer's noise. The values  $\sigma_w$ ,  $\sigma_{b1}$ , and  $\tau$  characterize the values of  $v_w$ ,  $\omega$ , and  $\tau$  in the sensor noise model [1].

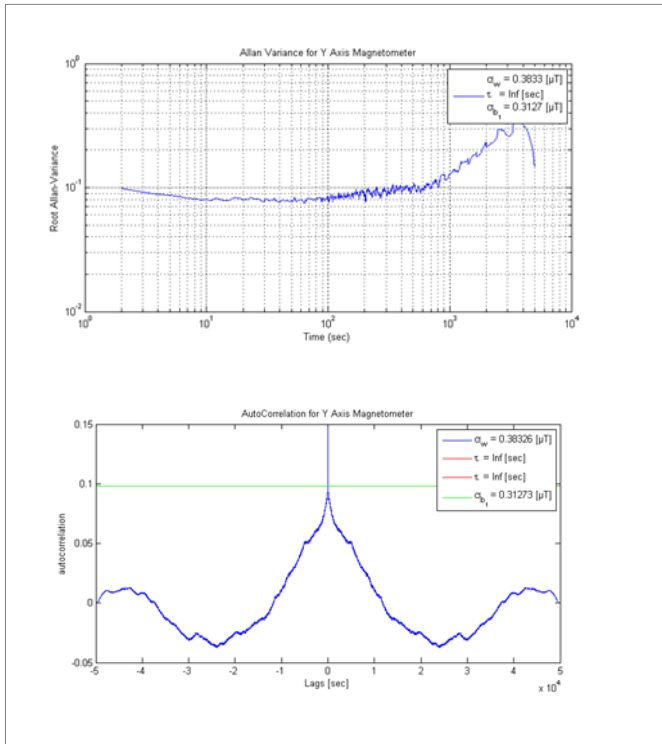


Fig. 2. These plots generated in analyzing signals from the magnetometer were much less useful. The plots (especially the autocorrelation plot) show that the data was correlated.

This is due to the fact that the magnetometer readings were correlated with temperature in a relatively linear relationship (Fig. 3). The linear relationship was characterized and the magnetometer data was corrected (Fig. 4). However, even the corrected data was not free from correlation, and the overbounding method remained not useful. This is most likely due to noise from the temperature sensor. In the future, a similar test should be run with a higher quality temperature sensor to fully characterize the noise of the magnetometer.

Table 1 displays the average values of the parameters of the noise models for each axis of the two sensors.

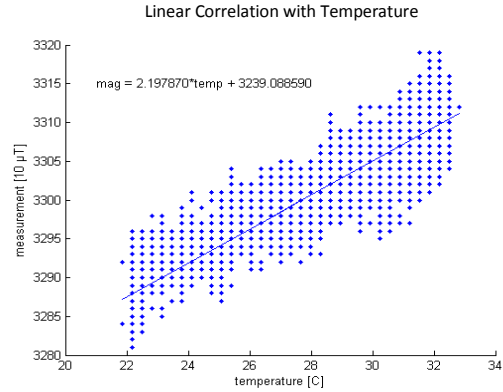


Fig. 3. This plot compares magnetometer sensor readings with temperature, showing the clear linear relationship between the two.

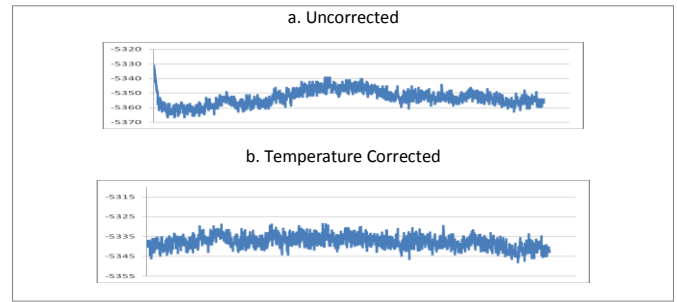


Fig. 4. These graphs show both uncorrected (a) and corrected (b) magnetometer data. The Y-axis is raw sensor output in bit counts and the X-axis is time, spanning a few hours.

TABLE I.

	$\sigma_w$	$\sigma_b$	$\tau$
acc <sub>x</sub>	0.6 mg	0.1 mg	98 s
acc <sub>y</sub>	0.6 mg	0.1 mg	122 s
acc <sub>z</sub>	0.7 mg	0.1 mg	112 s
mag <sub>x</sub>	2.2 $\mu$ T	2.4 $\mu$ T	n/a
mag <sub>y</sub>	2.5 $\mu$ T	2.4 $\mu$ T	n/a
mag <sub>z</sub>	4.3 $\mu$ T	3.1 $\mu$ T	n/a

Fig. 5. This table shows the averages of the values of  $\sigma_w$ ,  $\sigma_{b1}$ , and  $\tau$  from both overnight trials.

### III. STARTUP TIMES

When running the device, the various sensors will be power cycled to minimize battery usage and maximize the length of deployment. It is therefore important to understand the sensors' startup times: the time it takes from power on to stability. There are two motivations for this – first, to ensure data integrity by waiting the appropriate amount of time after powering on and second, to estimate and minimize power consumption.

The time for a GPS to find a fix has previously been characterized[2]. Tests to determine startup times of the magnetometer and accelerometer had several steps. First, the sensors were turned off – either by removing a power source or by turning the sensor to standby mode via I2C. Then, the sensors were moved into a different position to ensure that the post-restart readings would not be a memory of past readings. Lastly, the sensors were turned back on and/or to active mode. Immediately, data was recorded at 8 times the output data rate of the sensors. Trials were run at several of the sensor's output data rate settings – 6.25 Hz to 200 Hz on the accelerometer and 2.5 Hz to 80 Hz on the magnetometer.

Graphing the sensors' output against time reveals an obvious startup error, displayed in Fig. 6. To identify the time of stability in a consistent manner, the distribution of the last three quarters of data was used. Since stability was generally reached within the first two percent of the data, using the last three quarters as a comparison was fairly reliable. The first stable point was determined as being the first point to fall within 1.5 standard deviations of the stable data.

The time of the first stable point varied with output data rate setting. In Fig. 7, the times are plotted in terms of the output data rates, or in number of sampling periods. In most cases, it took at most two sampling periods to achieve stability.

### IV. POWER CONSUMPTION

#### A. Magnetometer and Accelerometer

To estimate length of deployment, it is necessary to understand the power consumption of the sensor. Therefore, the current draws of the accelerometer, the magnetometer, and the GPS were measured.

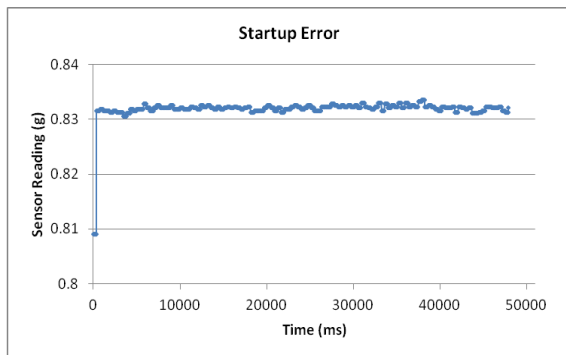


Fig. 6. Data from a freshly powered on sensor. Note the obvious startup error.

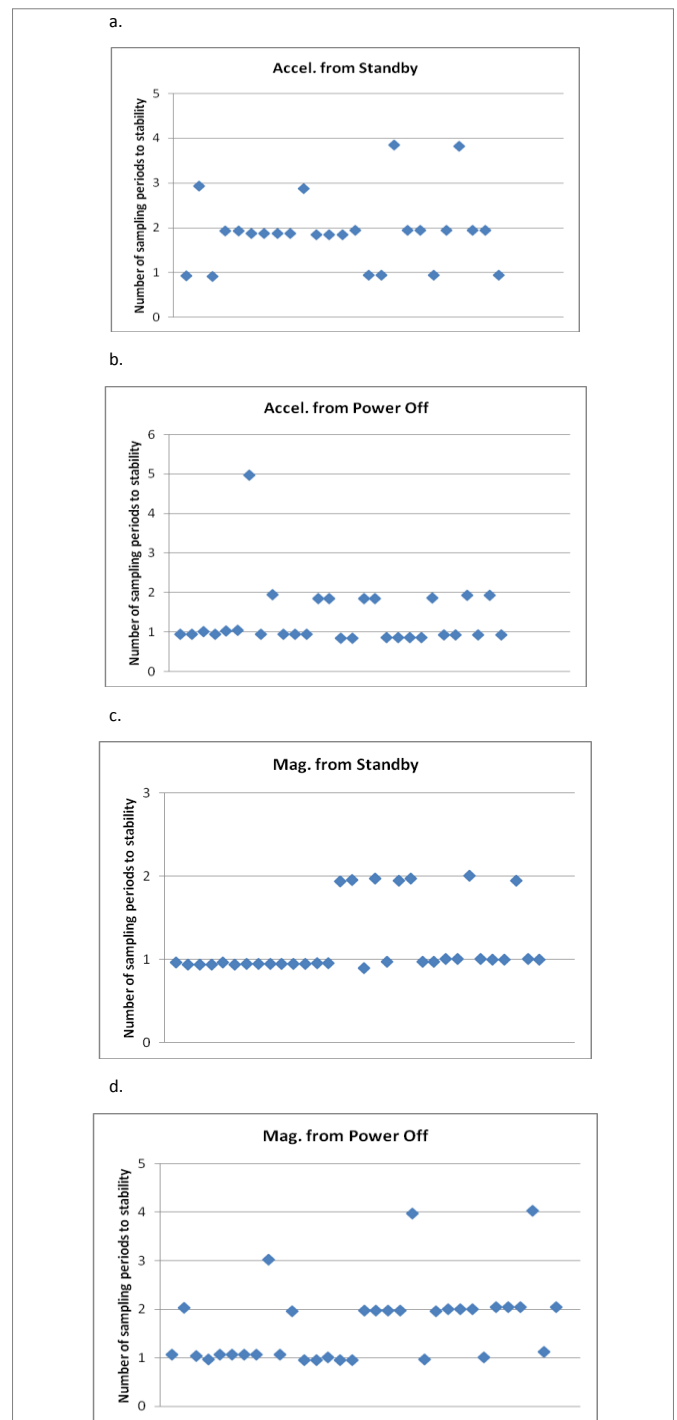


Fig. 7. Time of stability plotted in terms of sampling period for both the magnetometer (c, d) and accelerometer (a, b).

The current draws of the accelerometer and the magnetometer were characterized using a low side current sensing circuit. This was done with a TI INA212 current shunt monitor, which has a gain of 1000. The shunt resistor used was 1 ohm for the magnetometer and 4.7 ohms for the accelerometer.

The current draws for both sensors were characterized both in active and standby modes. For each sensor in active mode, the current was characterized for several of the various output data rate settings.

The current draw varied with the output data rate setting (Fig. 8 and Fig. 9), as was expected based on the data sheets. The accelerometer's measured current was consistently 20  $\mu\text{A}$  higher than the data sheet value for both active and standby modes (Fig. 8). Though 20  $\mu\text{A}$  is very small, the constant offset suggests a flaw in the measuring set up.

The magnetometer included settings for both output data rate and oversampling rate. The internal sample rate is OS multiplied by ODR, and this was the value that showed a correlation with current draw (Fig. 9). Again, there was a 20-25  $\mu\text{A}$  offset obvious in standby mode current draws.

Though the average current draws were generally consistent with the data sheet's values, there was much variation in the current draw when the sensors were in active mode (Fig. 10). Both the magnetometer and the accelerometer displayed this pattern of skewed current distributions in active mode. The distributions are displayed as cumulative density function graphs in Appendix A.

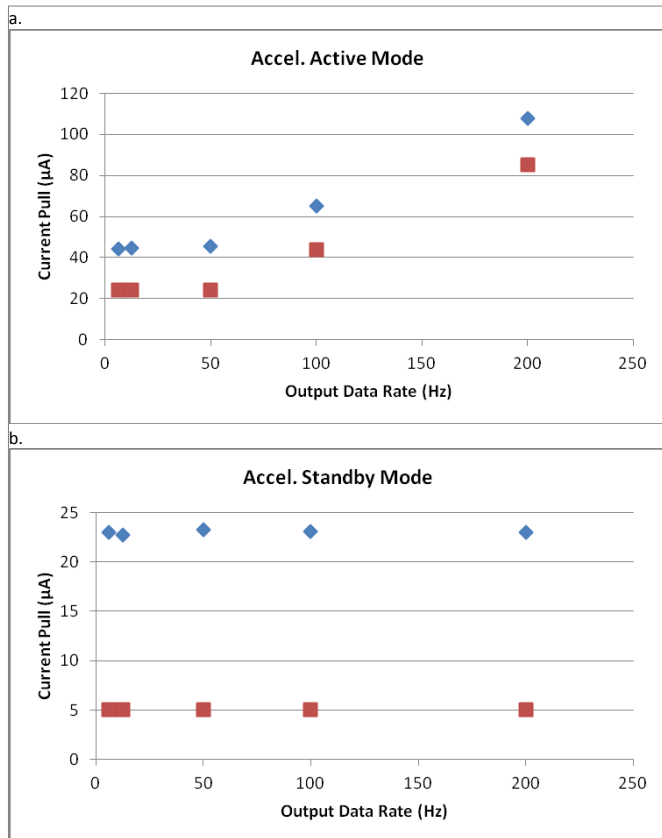


Fig. 8. The average current draw of the accelerometer at different Output Data Rate settings in both active (a) and standby (b) mode. The red points represent the values cited on the datasheet.

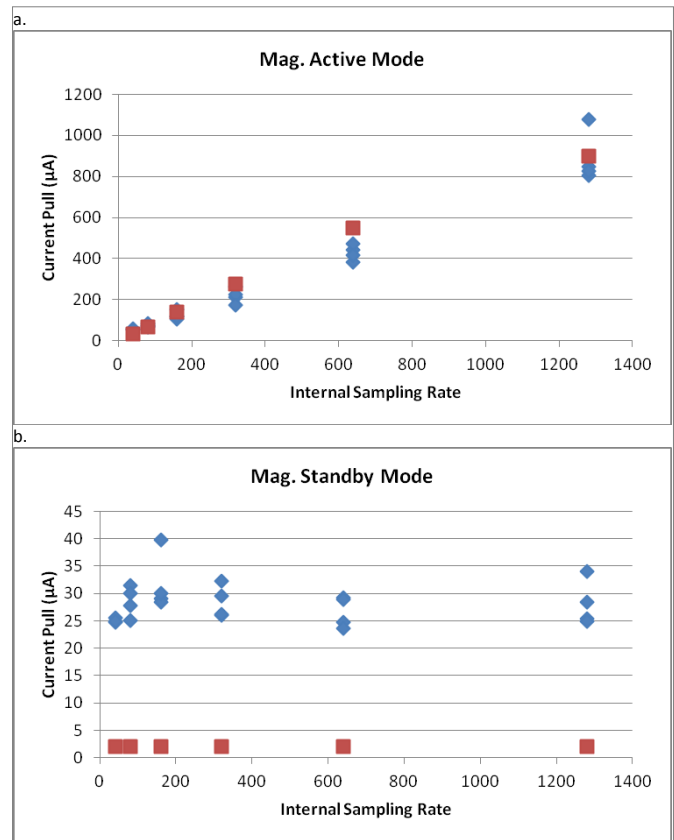


Fig. 9. The average current draw of the magnetometer at different internal sampling period (Output Data Rate \* Over Sampling ratio) settings in both active (a) and standby (b) mode. The red points represent the values cited on the datasheet.

## B. GPS

The current draw of the GPS was characterized using a low side current sensing circuit. This was done with two chained op-amps and a 1 ohm shunt resistor. The current draw was characterized while the GPS was acquiring a fix after a power on, a cold restart, a warm restart, and a hot restart. These restart types simulate the GPS starting with different amounts of information about its location. The time to acquire a fix is known to vary between the different restarts[2].

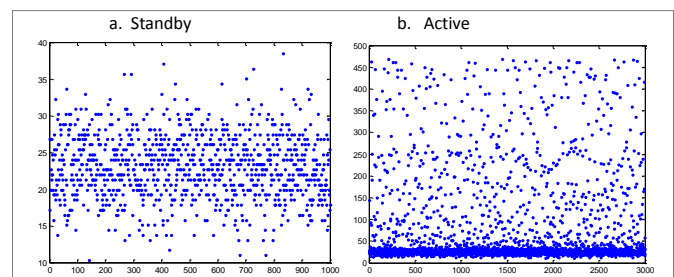


Fig. 10. An example sample of raw current draw data of the accelerometer's current draw in both standby (a) and active (b) mode. Note the normal distribution of the standby data (a) in contrast with the skewed distribution of the active data (b).

The average measured currents of the GPS are displayed in Fig. 11. Oddly, there is a noticeable difference in the current draw between the post-turn on and post-cold restart. A cold restart is meant to simulate the GPS turning on from power off. This difference draws into suspicion the restart functions of the GPS. However, an important observation remains: the average current draw varies very little between the different types of restarts. Further tests should be done to understand the discrepancy between the post-turn on current and the post-cold restart current.

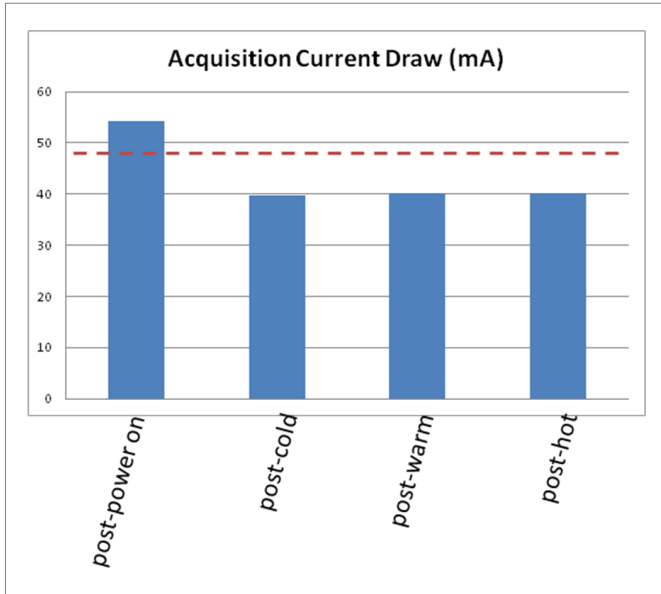


Fig. 11. The average current draw of the accelerometer at different Output Data Rate settings in both active (a) and standby (b) mode. The red line represents the current draw cited in the datasheet. A.

Like the magnetometer and the accelerometer, the GPS showed a skewed distribution of current draws. The distribution is also displayed in cumulative density function graphs in Appendix A.

## CONCLUSIONS

The characterizations of the magnetometer, accelerometer, and GPS done in this project will be valuable to the ANIMA project at UC Santa Cruz. Using the information about stability, the sensor's noise can be modeled and data processing algorithms can be refined. Using the startup and power consumption information, a power aware state machine can be create that cycles power to the sensors in the most energy efficient way. Furthermore, the sensors may be used in other projects, so the characterization of them will be useful.

## ACKNOWLEDGMENTS

SD would like to thank the members of the Autonomous Systems Lab at UCSC, especially graduate student Max Dunne and Dr. Gabriel Elkaim. SD's work was supported by the SURF-IT REU internship, which is funded by the National Science Foundation.

## REFERENCES

- [1] Xing Zhiqiang, Gebre-Egziabher D, "Modeling and bounding low cost inertial sensor errors," *IEEE/ION PLANS 2008 - Position, Location and Navigation Symposium*, Monterey, California, 2008.
- [2] M. Dunne, private communication, August 2013.

## APPENDIX A

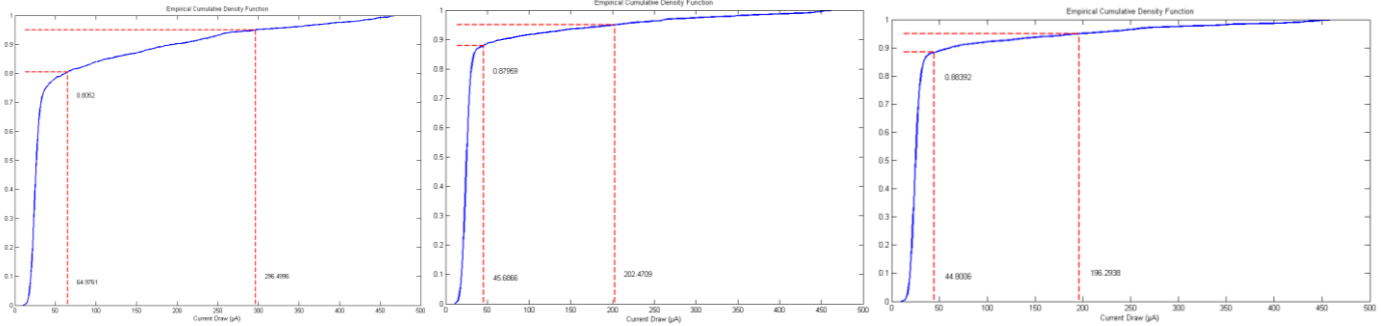
Displayed below are graphs of the empirical average cumulative density functions of the current draws of the sensors at different sampling rates. Indicated by red lines on the graphs are the average current draws and the current under which the sensor drew 95% of the time. Also denoted is the percentage of current draws under the average current draw.

### Accelerometer

6.25 Hz

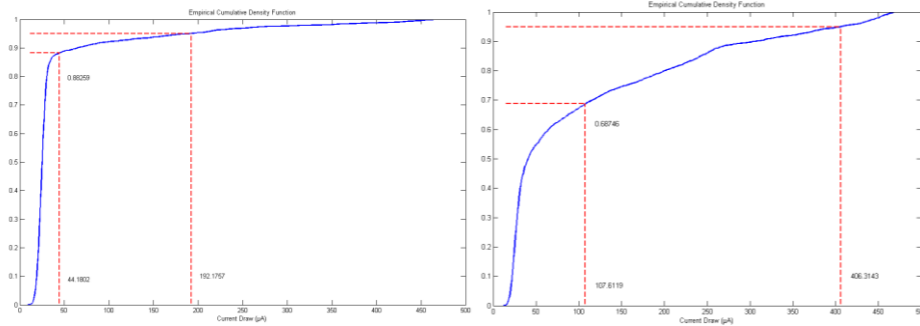
12.5 Hz

50 Hz



100 Hz

200 Hz

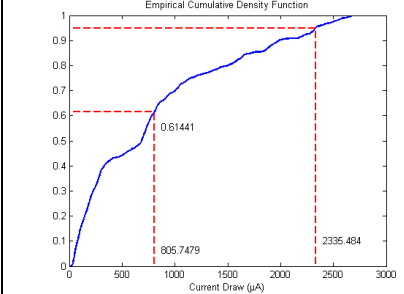
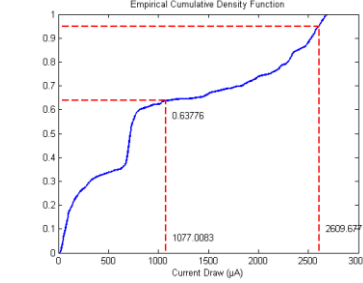
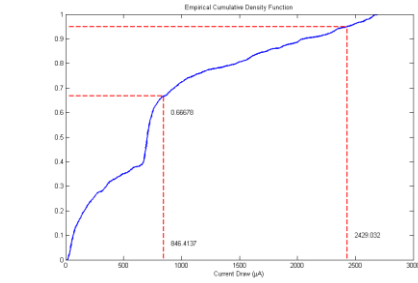


### Magnetometer

ODR: 80 Hz, OS: 16

ODR: 40 Hz, OS: 32

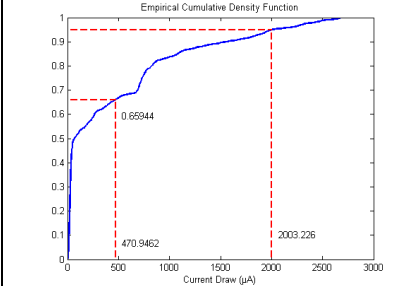
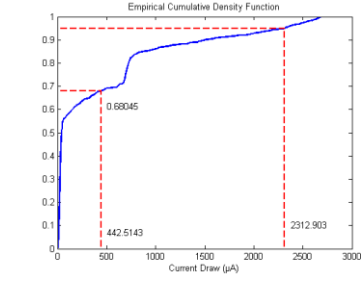
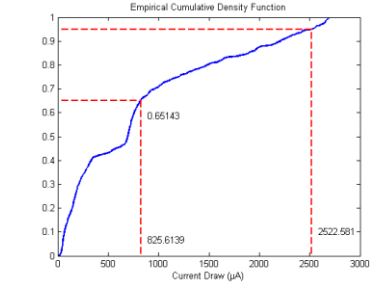
ODR: 20 Hz, OS: 64

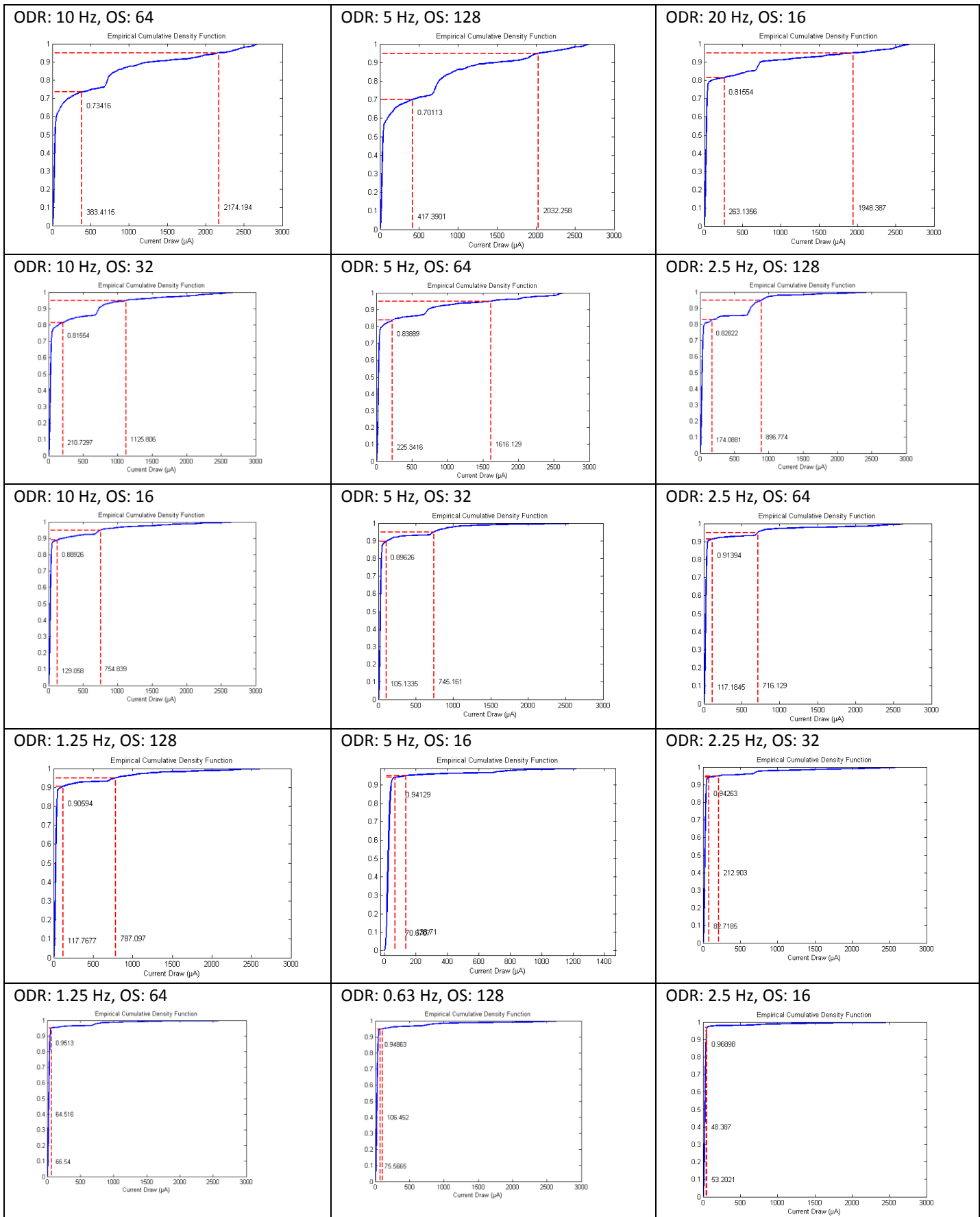


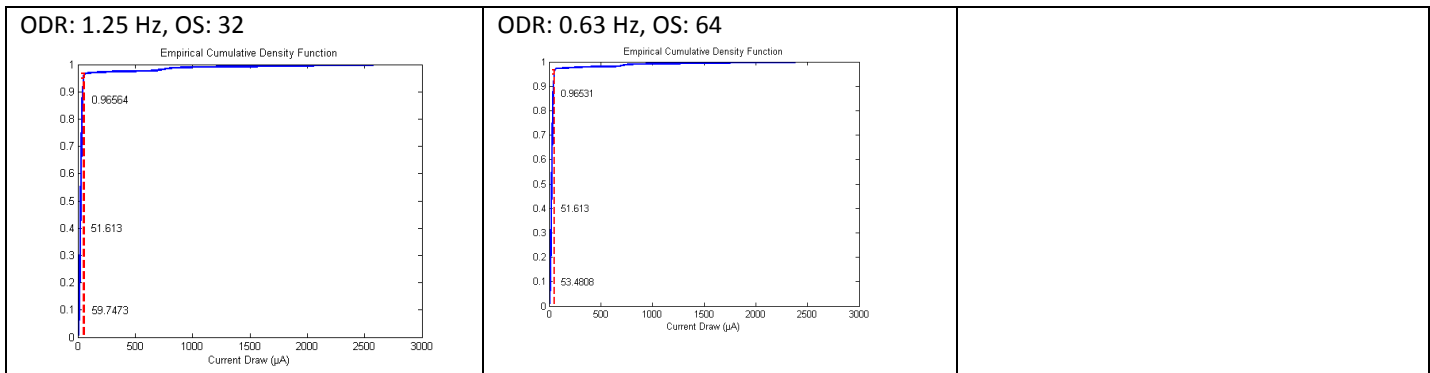
ODR: 10 Hz, OS: 128

ODR: 40 Hz, OS: 16

ODR: 20 Hz, OS: 32

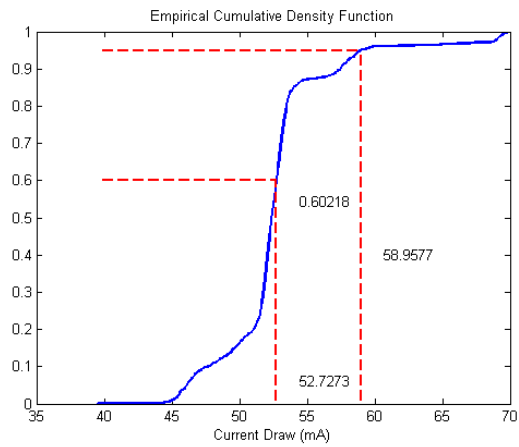




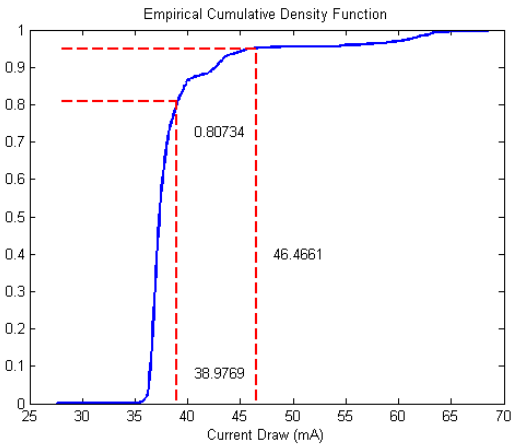


**GPS**

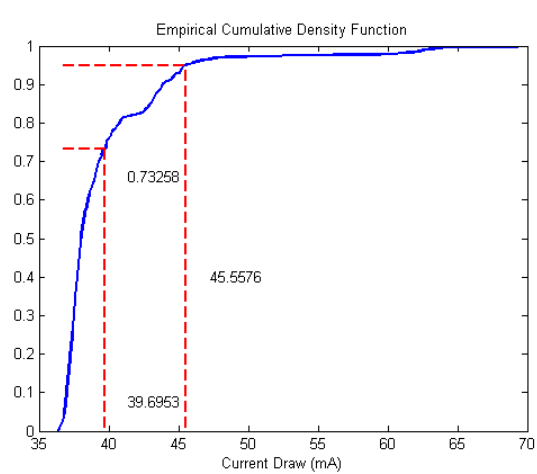
**Post-Power On**



**Post-Cold Restart**



**Post-Warm Restart**



**Post-Hot Restart**

